

## New wave effects in nonstationary plasma<sup>a)</sup>

P. F. Schmit<sup>1,b)</sup> and N. J. Fisch<sup>2</sup>

<sup>1</sup>Sandia National Laboratories, P.O. Box 5800, Albuquerque, New Mexico 87185-1186, USA

<sup>2</sup>Department of Astrophysical Sciences, Princeton University, Princeton, New Jersey 08544, USA

(Received 14 December 2012; accepted 30 January 2013; published online 16 April 2013)

Through particle-in-cell simulations and analytics, a host of interesting and novel wave effects in nonstationary plasma are examined. In particular, Langmuir waves serve as a model system to explore wave dynamics in plasmas undergoing compression, expansion, and charge recombination. The entire wave life-cycle is explored, including wave excitation, adiabatic evolution and action conservation, nonadiabatic evolution and resonant wave-particle effects, collisional dissipation, and potential laboratory applications of the aforementioned phenomenology. © 2013 AIP Publishing LLC  
[\[http://dx.doi.org/10.1063/1.4801747\]](http://dx.doi.org/10.1063/1.4801747)

### I. INTRODUCTION

Waves have enjoyed a long and diverse history as a useful, and sometimes even critical, tool in the design and operation of magnetic fusion experiments. In magnetically confined fusion plasmas, a variety of waves are supported that exhibit resonance mechanisms allowing for the efficient exchange of energy and momentum between a wave and specific populations of charged plasma constituents. The utilization of wave-particle interactions in magnetic fusion has yielded remarkable surges in technological capabilities and system performance. For example, waves are used for such tasks as heating the plasma,<sup>1–3</sup> driving electrical current to create confining magnetic fields,<sup>4,5</sup> and even channeling the energy of fusion byproducts to fuel ions, while simultaneously exhausting byproducts to the system periphery.<sup>6–10</sup>

Despite the rapid advancements made in the world's most sophisticated and powerful inertial confinement fusion (ICF) experiments, such as NIF<sup>11,12</sup> and Z,<sup>13–15</sup> a commensurate understanding of the role played by wave-particle interactions in the high energy density (HED), highly nonstationary environments characteristic of such experiments is notably lacking. Neither have kinetic wave-particle interactions been considered an essential feature of basic ICF target implosion physics nor has the existence of such interactions been recognized as an ideal platform to perform useful tasks, in stark contrast with other approaches to fusion. On the other hand, much scientific interest exists in kinetic plasma processes associated with nonstationary astrophysical plasmas, such as solar flares<sup>16–19</sup> and cosmic ray sources,<sup>20,21</sup> as well as with plasmas occurring in the vicinity of nuclear explosions.<sup>22,23</sup> Thus, the ubiquity of nonstationary plasma throughout terrestrial and astrophysical plasma systems indicates that the field is ripe for an exploration of kinetic wave dynamics in such environments.

Here, we review a number of recent results of our investigation of wave dynamics in nonstationary plasma and offer a broad, more complete account of the impact of these new concepts afforded by the perspective taking into account the

entire body of work. In plasma undergoing compression, embedded waves can have very unusual and possibly useful properties. For example, part of the mechanical energy of compressing plasma can be transferred controllably to hot electrons by seeding the plasma with plasma waves. Under compression, wherein wave action is conserved, the wave energy grows as its frequency and wavenumber change adiabatically, until, suddenly, the wave damps, resulting in switchlike production not only of heat but also voltage and current. These bursts can be controlled precisely in time by prescribing the compression script. Several classic problems in wave physics, including the bump-on-tail instability, nonlinear Bernstein-Greene-Kruskal (BGK) wave dynamics, and collisional relaxation, exhibit new effects under compression, expansion, and charge recombination. In addition, waves affect fundamental properties of plasma undergoing compression or expansion, such as the plasma compressibility; moreover, and rather remarkably, nonlinear waves, such as BGK modes, affect the plasma compressibility differently. Nonlinear BGK modes are also used to conduct the first *ab initio* test of a new theory of nonlinear wave action conservation.<sup>24</sup> Wave-particle interactions mediated by plasma compression also can enhance the performance of plasma-based particle accelerators. To describe numerically all these effects, novel particle-in-cell (PIC) simulations were developed. These findings point towards potentially beneficial applications, including in ICF and HED physics, where extreme compression is exercised on dense plasma, which could be seeded with waves.

The article is organized as follows. First in Sec. II, the PIC codes developed for this study are described briefly. In Sec. III, wave effects associated with bulk plasma motion parallel to the direction of wave propagation (*longitudinal* compression/expansion) are discussed. In Sec. IV, wave effects associated instead with plasma motion perpendicular to the direction of wave propagation (*transverse* compression/expansion) are discussed. Section V explores two possible laboratory applications—current drive and plasma-based particle acceleration—both of which exploit the unique wave behavior observed in nonstationary plasma. Section VI presents a summary of our results.

<sup>a)</sup>Paper UI2 2, Bull. Am. Phys. Soc. 57, 339 (2012).

<sup>b)</sup>Invited speaker.

## II. SIMULATING WAVES IN NONSTATIONARY PLASMA

In order to simulate wave evolution in compressing plasma, a PIC code was developed capable of modeling electrostatic plasma physics in one spatial dimension (1D) and two velocity dimensions (2V), i.e., velocities parallel ( $v_{\parallel}$ ) and perpendicular ( $v_{\perp}$ ) to the spatial dimension being simulated. Langmuir waves serve as the paradigmatic wave phenomenon to be studied quantitatively, and both linear and nonlinear Langmuir waves can be excited in the PIC simulations through embedded perturbations, plasma instabilities, or applied external potentials. The exact nature in which different waves are generated will be explained in each section that follows.

A Fokker-Planck collision algorithm based on Ref. 25 is included to provide a mechanism coupling  $v_{\parallel}$  and  $v_{\perp}$ . This particular algorithm was chosen due to its time-explicit formulation, straightforward implementation, good numerical stability properties, and, most importantly, its preservation of the  $1/v_{\text{rel}}^3$  scaling of charged particle collisionality, where  $v_{\text{rel}}$  is the magnitude of the relative velocity between two charged particles. This is crucial, considering some important effects that we investigate, such as wave-based current drive, rely heavily on the anisotropic collisional relaxation of a distribution of electrons driven resonantly by waves in a preferred direction. As suggested in Ref. 25, a  $\delta$ -function kernel is adopted in the collision integral, which reduces the random number generation requirement to only one per binary collision, and still converges to the exact Landau-Fokker-Planck result with  $\mathcal{O}(\Delta t)$  accuracy. This algorithm is certainly not the only one that could have been chosen, as there is a rapidly growing body of literature seeking to develop increasingly stable and efficient PIC collision models; e.g., Refs. 26–30. Nevertheless, the charged particle scattering algorithm developed in Ref. 25, and an earlier, related method developed in Ref. 31, have both received particular attention from within the field resulting, e.g., in at least two recent external evaluations in the peer-reviewed literature.<sup>32,33</sup>

Electrons are initialized generally as Maxwellian, perhaps with an initial perturbation, while ions either can be modeled kinetically as well, or they can be treated as a uniform charge-neutralizing background. The code employs an FFT electrostatic field solver and a leapfrog particle mover, the latter chosen for its efficiency, simplicity, and its preservation of symplectic structure. The essential architecture and routine functions of the PIC code follow well-established principles, most of which are explained in detail in the definitive Ref. 34. On the other hand, the unique features of the code primarily reside in how bulk nonstationary effects are modeled (discussed below).

The primary purpose of the PIC code is to capture quantitatively the dynamical evolution of embedded waves in the presence of compression and expansion of the bulk plasma; as such, nonstationary bulk evolution is accomplished through two separate means. To simulate longitudinal compression or expansion of the plasma (with respect to the direction of wave propagation), perfectly reflecting, non-absorbing hard walls are placed at the boundaries of the simulation domain, and one of the walls is given a smooth,

programmable velocity profile, acting like a piston on the plasma. On the other hand, transverse compression or expansion is modeled by employing periodic boundary conditions parallel to the direction of wave propagation, while the mass and charge of the PIC particles are rescaled as a function of time. By keeping the PIC particle charge-to-mass ratio fixed, rescaling effectively simulates the redistribution of charge across the perpendicularly homogeneous charge sheets modeled by the 1D PIC code. In the event that transverse compression or expansion is intended to be produced by the adiabatic modulation of a uniform longitudinal magnetic field of strength  $B(t)$ , which does not directly affect parallel particle dynamics, the effect of the slowly changing magnetic field is captured by a numerical routine that enforces the conservation of the particle magnetic moment,  $\mu \propto v_{\perp}^2/B$ , on very short time scales,  $\Delta t$ ; i.e.,  $\Delta\mu = 0$ . The collisional subroutine then can violate  $\Delta\mu = 0$ , but on such short time scales, the two effects can be considered additive. Thus, the combination of  $\mu$ -conservation and collisions effectively couples parallel and perpendicular velocities providing, e.g., additional sources and sinks for the energy of embedded waves. Here, we presume  $\Delta t \ll \omega_p^{-1} \ll \nu_e^{-1}$ , where  $\omega_p^2 = 4\pi n_e e^2/m_e$  is the electron plasma frequency,  $n_e$  is the electron number density, and  $\nu_e$  is the electron collision frequency.

The intent of these simulations is to provide an ideal numerical laboratory to isolate and diagnose key nonstationary wave phenomena, while simultaneously avoiding additional effects and complications associated with finite plasma extent, device-like interactions with boundaries, and higher dimensional considerations. As such, the exact nature of the compression or expansion often can be considered inessential, arising, e.g., due to ballistic plasma motion or a time-varying magnetic field. Anisotropy-driven instabilities,<sup>35–38</sup> which could invalidate this assumption for some physical systems, are assumed negligible on the compression or expansion time scale, and some effort is made to establish fairly general constraints to ensure fidelity of the physical model.

Through the various tools and simplifications incorporated into the PIC code, the simulations capture many essential effects of wave evolution in nonstationary plasma in a framework that improves drastically the economy and efficiency of the code. The simulation results and their theoretical interpretations will be presented in the sections that follow.

## III. LONGITUDINAL NONSTATIONARY PLASMA EFFECTS

### A. Adiabatic linear wave evolution and threshold dynamics

An initially cold plasma wave embedded in plasma undergoing densification and heating evolves adiabatically at first, but after some time, a sudden transition can occur in which resonant wave-particle interactions and nonadiabatic dynamics become significant. The nature of this transition from a cold plasma regime to a hot plasma regime can be characterized well in the case of a 1D plasma undergoing longitudinal, piston-like compression.<sup>39</sup>

Consider a linear wave immersed in collisionless plasma and far from any collisionless resonances. Under such

conditions, a linear wave will not (at first) experience dissipation, and thus, the wave action,  $I$ , is conserved for slow, adiabatic compression or expansion of the bulk plasma.<sup>24,40–45</sup> The action conservation theorem (ACT), which holds generally for any linear wave, is given by

$$I = \int_{\mathcal{V}} (\mathcal{W}/\omega) d\mathcal{V}, \quad (1)$$

$$= \text{const},$$

where  $\mathcal{W}$  is the (local) linear wave energy density,  $\omega$  is the (local) wave frequency, and the integral is taken over the plasma volume,  $\mathcal{V}$ . In the case of a linear Langmuir wavepacket, adiabaticity requires  $\kappa \equiv k\lambda_D \ll 1$ , where  $k$  is the longitudinal wavenumber,  $\lambda_D = v_{Te}/\omega_p$  is the Debye length, and  $v_{Te}$  is the electron thermal velocity. Such a constraint minimizes the impact of Landau damping, which introduces dissipation and thus breaks the ACT. To extract quantitative predictions from Eq. (1), one also has for linear Langmuir waves  $\mathcal{W} = 2\Omega^2\mathcal{W}_E$ ,  $\Omega \equiv (1 + 3\kappa^2)^{1/2} \approx 1$ , and  $\mathcal{W}_E = E^2/(16\pi)$ ,<sup>44</sup> where the latter quantity is the electrostatic component of the total wave energy density.

For longitudinal compression, one has  $\mathcal{V} = \epsilon \times \text{const}$ , where  $\epsilon \equiv L/L_0$  is the normalized length of the plasma, and the subscript 0 henceforth refers to initial conditions. In terms of  $\epsilon$ , the system parameters scale as follows:  $\omega_p \propto \epsilon^{-1/2}$ ,  $k \propto \epsilon^{-1}$ ,  $v_{Te} \propto \epsilon^{-1}$ , and thus,  $\kappa \propto \epsilon^{-3/2}$ . (See Ref. 39 for a more detailed explanation of these scalings.) Hence, Eq. (1) yields  $G = \bar{\Omega}^{-1}\epsilon^{-3/2}$ , or in terms of the normalized density,  $N \equiv n/n_0 \propto \epsilon^{-1}$ ,

$$G = \bar{\Omega}^{-1}N^{3/2}, \quad (2)$$

where the amplification gain  $G \equiv \mathcal{W}_E/\mathcal{W}_{E0}$ ,  $\bar{\Omega} \equiv \Omega/\Omega_0$ , and  $\Omega = (1 + 3\kappa_0^2N^3)^{1/2}$  for longitudinal compression or expansion. Thus, the ACT predicts the wave electrostatic energy density amplifies with compression until the assumption of adiabaticity is violated.

With further compression, the condition  $\kappa \ll 1$  is no longer satisfied, as the wave phase velocity,  $u = \omega/k \propto N^{-1/2}$ , is slowing down with densification, while  $v_{Te} \propto N$  implies electrons are absorbing energy, which eventually must lead to collisionless wave dissipation. In Ref. 39, a geometrical optics approach is employed to predict the *switchlike* onset of Landau damping, in which the scaling of the linear Landau damping rate with compression due to the slowly evolving plasma parameters follows from the expression<sup>46</sup>

$$\gamma_L \approx \frac{\omega_p}{\kappa^3} \sqrt{\frac{\pi}{8}} \exp\left(-\frac{1}{2\kappa^2} - \frac{3}{2}\right). \quad (3)$$

Then, damping causes exponential decay of the wave action,  $I = I_0 \exp(-2\Gamma)$ , where  $\Gamma = \int_0^t \gamma_L(t') dt'$ . A generalization of Eq. (2) follows by including this exponential decay, i.e.,

$$G' = \bar{\Omega}^{-1}N^{3/2} \exp(-2\Gamma). \quad (4)$$

As a result of sudden collisionless damping, electrons resonant with the amplified wave are carried, on average, to

higher energies, resulting in an enhanced non-thermal high energy component of the electron distribution function. This enhanced tail carries most of the energy initially found in the bulk oscillations supporting the wave, which is amplified further through mechanical compression prior to Landau damping.

Both the linear ACT and sudden transition into a collisionless damping regime are confirmed in PIC simulations, where 1D longitudinal compression is simulated in a plasma bounded by perfectly reflecting hard walls, one of which is given a smooth velocity profile,  $V(t)$ , with  $|V| \ll v_{Te}$ .<sup>39</sup> Figure 1 shows the results of a typical simulation, with clearly delineated regimes showing initial action conservation followed by a sudden transition into collisionless damping, until all wave energy has been removed from the system. The analytical prediction, corresponding to Eq. (4), predicts the adiabatic amplification well. The slightly delayed onset of damping of the simulated wave relative to the analytical prediction is thought to arise from the incomplete resolution of the high energy tail of the Maxwellian, typical in PIC simulations. In addition, the necessarily slow compression of the plasma implies that the wave is in the trapping regime,<sup>47</sup> in which the compression rate,  $\eta \equiv V/L$ , obeys the ordering  $\eta \ll \gamma_L \ll \omega_b$ , where  $\omega_b = (eEk/m_e)^{1/2}$  is the electron bounce frequency, with  $E$  the electric field amplitude. In this case,  $\gamma_L$  is smaller than predicted by Eq. (3), also implying slower decay of the wave than predicted by the linear theory. Nevertheless, the results indicate

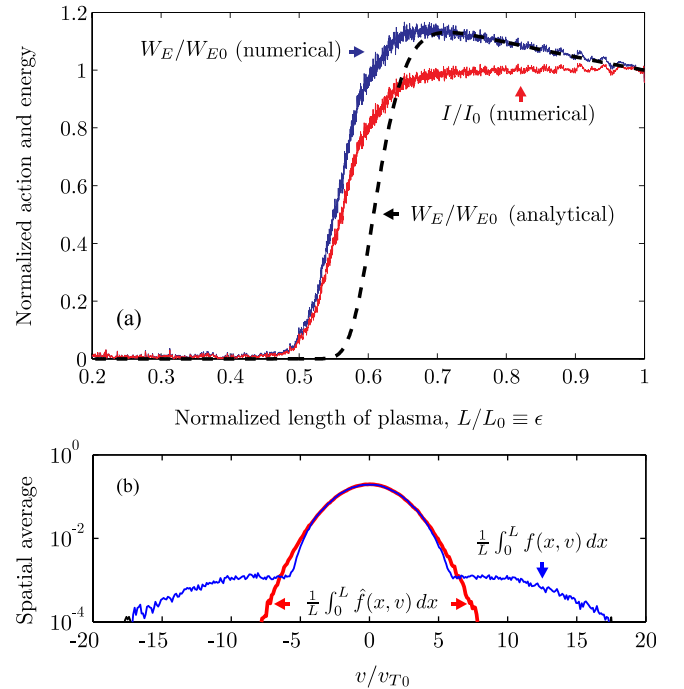


FIG. 1. (a) The normalized total action,  $I/I_0$ , and total electrostatic energy,  $W_E/W_{E0}$ , for an initially undamped Langmuir wave in plasma undergoing longitudinal compression. The analytical plot corresponds to  $G'/N$  (cf. Eq. (4)). (b) The electron distribution function compressed together with a wave,  $f(x, v)$ , and the same distribution function compressed without the wave,  $\hat{f}(x, v)$ , showing the production of suprathermal electrons. Figure from Ref. 39. Reprinted with permission from P. F. Schmit, I. Y. Dodin, and N. J. Fisch, Phys. Rev. Lett. **105**, 175003 (2010). Copyright 2010 American Physical Society.

a substantial degree of predictability of the switchlike damping effect both by numerical and analytical means.

While the numerical results presented above pertain specifically to linear Langmuir waves undergoing longitudinal compression, the underlying ACT and threshold behavior near the onset of collisionless damping is sufficiently general to be applied to a wide variety of systems. The practical interest in such effects arises then from the notion that waves in nonstationary plasma can act as embedded switches, which could be used to heat individual particle populations or drive electrical currents at predetermined instants during the bulk plasma evolution. Indeed, the terminal electron distribution function observed in Fig. 1 clearly indicates the effect of the damped standing wave structure excited in the simulation, namely, an accentuated isotropic, non-thermal electron tail population. Thus, some fraction of the mechanical energy of compression, which is channeled into the amplifying standing wave structure due to the ACT, is then deposited onto a specific particle population, in this case suprathermal electrons, in a targeted and predictable manner.

Further discussion on this topic can be found in Ref. 39.

## B. Bump-on-tail instability and plasma compressibility

The well-known bump-on-tail instability (BoTI) demonstrates increasingly complex dynamical wave behavior in nonstationary plasma, as one transitions from the consideration of a single linear monochromatic wave or single wavepacket to the broadband resonant, stochastic, *nonlinear* interactions characteristic of the instability.<sup>48</sup> Numerical PIC studies of bump-on-tail unstable plasma subject to longitudinal compression shed light on two interesting and related concepts: first, the final plasma state in the presence of BoTI differs from that described by quasilinear theory for stationary bulk plasma and can depend on the compression history, and second, the transformation of bulk thermal energy into wave energy by the BoTI increases the bulk plasma compressibility.

Consider the plasma total energy,  $U$ , as the sum of the wave total energy,  $W$ , and the thermal total energy,  $W_T$ , for which there is a unique decomposition,  $U = W + W_T$ .<sup>49</sup> Since BoTI conserves total energy, it cannot change  $U$ , but it can change the instantaneous ratio  $\rho \equiv W/U = 1 - W_T/U$ . Remarkably, this affects the plasma pressure,<sup>50</sup> defined as usual through  $\mathcal{P} = -dU/d\mathcal{V}$  for adiabatic compression, and also the energy gain,  $\Delta U$ , through compression. From the standpoint of quasilinear theory,<sup>51</sup> the BoTI drives a broadband spectrum of linear Langmuir waves resonant with the electron population inversion in velocity-space, and thus, according to the scalings described above, one has  $W \propto \mathcal{V}^{-1/2}$  and  $W_T \propto \mathcal{V}^{-2}$ . Hence,  $dW = -Wd\mathcal{V}/(2\mathcal{V})$ ,  $dW_T = -2W_Td\mathcal{V}/\mathcal{V}$ , and

$$\mathcal{P} = 2\mathcal{U}(1 - 3\rho/4), \quad (5)$$

where  $\mathcal{U} \equiv U/\mathcal{V}$  is the average total plasma energy density. Since BoTI cannot affect  $\mathcal{U}$  but increases  $\rho$  (at least

temporarily), it thereby decreases  $\mathcal{P}$ . Therefore, considering the definition of the plasma compressibility,<sup>52</sup>  $\beta_S \equiv -(1/\mathcal{V})d\mathcal{V}/d\mathcal{P}$ , or  $\beta_S = 1/\mathcal{P}$  here, one finds that the conversion of thermal energy to wave energy (by BoTI or some other means) *increases* the plasma compressibility. The subscript  $S$  indicates here that we are referring to the adiabatic, or isentropic, compressibility of the plasma. Additionally, the total energy gain,  $\Delta U = \int \dot{U} dt$ , can be calculated using  $\dot{U} = 2U[1 - 3\rho(t)/4]\eta(t)$ , where the compression rate  $\eta \equiv -\dot{\mathcal{V}}/\mathcal{V}$  has been introduced. Thus, one also finds that  $\Delta U$  is decreased by the influence of the BoTI.

The function  $\rho(t)$  varies depending on the manner in which BoTI developed during compression. Thus,  $U$  is *not* a function of the plasma volume and, in this sense, is not a state variable, unlike for a neutral gas or plasma containing only nonresonant, dissipationless waves. This is because the latter cases can be thought of as systems containing a large number of degrees of freedom, both particle-like and collective, in thermodynamic equilibrium, while the system undergoing BoTI contains several *nonequilibrium* collective degrees of freedom that are resonantly coupled both to each other and to the bulk plasma “thermal reservoir.” Thus, the sensitivity of the evolution of BoTI to the time history of compression results in a continuum of possible  $\Delta U$ .

Interestingly, the theoretically maximum free energy available through velocity-space instabilities by evolution of the Vlasov equation, namely, the free energy available under so-called *Gardner restacking*,<sup>7,53,54</sup> is unaffected by the details of the compression. Since adiabatic compression drives a self-similar evolution of the particle velocity distributions, restacking prior to compression or subsequent to compression yields the same final distribution and liberates the same amount of particle energy. However, since wave-particle interactions generally act diffusively in plasma, the free energy that can be liberated by velocity-space instabilities must be further constrained by diffusive considerations. Constrain further the details of such diffusive behavior by invoking a particular compression script, and it becomes clear that the maximization of this free energy release, of practical interest, e.g., in the case of  $\alpha$ -channeling,<sup>6</sup> requires more information than just the initial particle and field configurations.

Further discussion on this topic can be found in Ref. 48.

## C. BGK mode evolution

Rather than the broadband, stochastic quasilinear dynamics associated with the BoTI, consider the strongly correlated nonlinearity associated with quasistatic, phase-mixed electron plasma wave equilibria, commonly termed *BGK modes*<sup>56,57</sup> or *electron holes*.<sup>58,59</sup> For such modes, a significant departure from the behavior associated with linear plasma waves is observed in the presence of nonstationary bulk plasma evolution.<sup>55</sup> Unlike linear waves, whose wavelength decreases proportionally to the system length,  $L(t)$ , nonlinear plasma waves are found to conserve their characteristic size,  $\Delta$ , during slow longitudinal compression by a perfectly reflecting wall. This has a dramatic effect on the

amplification of the wave with plasma densification, which is stronger than the amplification observed for linear waves.

In collisionless plasma, phase-mixed BGK equilibria are undamped, long-lived solitary structures exhibiting an electric potential that maintains its shape as the wave propagates, creating a suitable mechanism whereby the wave can retain a population of trapped electrons. In the context of longitudinal plasma compression, solitary nonlinear plasma waves are formed as the saturated state of a strong bump-on-tail instability, a well-documented phenomenon in unbounded plasma as well.<sup>60–65</sup> Figure 2 shows the development of a single solitary electron hole after the coalescence instability causes the nonlinear structures driven by the BoTI to merge.<sup>66,67</sup>

The amplification of a typical solitary nonlinear plasma wave subject to longitudinal bulk plasma compression is shown in Fig. 3. Compared to the peak amplification of a typical linear plasma wave by similar compression (cf. Fig. 1), total wave energy gains attainable through the amplification of nonlinear waves are regularly at least an order of magnitude larger. This feature is due to two factors: (i) nonlinear modes do not undergo linear Landau damping and (ii) their amplitude changes more rapidly with decreasing  $\epsilon$  (or increasing  $N$ ). The latter characteristic is due to the fact that the dynamics of a strongly nonlinear mode is determined primarily by phase-locked, resonant particles (cf. Ref. 68), which are absent in linear waves. The consequences of this strong dependence on the dynamics of trapped and nearly resonant particles are described heuristically as follows.

First, for most of the simulation, the relevant time scales are ordered as follows:  $\tau_r \ll \tau_b$ , where  $\tau_b = 2\pi/\omega_b$  is the characteristic bounce period of trapped electrons, and  $\tau_r \approx \Delta/u$  is the approximate time taken for the wave,

traveling at the nonlinear phase velocity  $u$ , to reflect off the wall. Thus, reflection occurs quickly relative to trapped particle bounce motion, implying trapped particles are essentially free-streaming on the  $\tau_r$ -time scale. Notice that the distance between two free-streaming particles with equal initial velocities is conserved upon reflection of both particles from a wall moving at constant velocity, since this distance is a Galilean invariant and obviously is conserved in the rest frame of the wall. The assumption of a nearly constant wall velocity assumes that  $V/\dot{V} \gg \tau_r$ . For the BGK mode, the velocity spread over the trapping island is sufficiently small to ensure that the distance is conserved between *all* trapped particles during reflection. As such, the mode shape is not substantially affected by moving walls, at least until the mode no longer fits in the system, which is related to the sudden damping observed in Fig. 3.

Thus, the approximate scaling behavior of the wave total energy can be deduced by the following argument. The electron density depletion due to the nonlinear mode results in an uncompensated background ion density  $\delta n_i$ . Assuming the electron hole charge is approximately fixed, one has  $\delta n_i \propto \epsilon^{-1}$ . The characteristic field of the hole is  $E \approx 4\pi\delta n_i\Delta$ , so conservation of  $\Delta$  yields the wave total electrostatic energy scaling  $W_E \propto \mathcal{W}_E\Delta \propto \epsilon^{-2}$ , which is reasonably close to the scaling observed in simulations [Fig. 3], though other fitting functions can describe slightly better the amplification curve. In comparison, the wave total electrostatic energy for a linear plasma wave subject to longitudinal compression is only  $W_E \propto \epsilon^{-1/2}$ . It should also be noted that, while the linear plasma wave energy scaling is derived from an ACT, the energy scaling for BGK modes is fundamentally *nonadiabatic*. Throughout the entire course of compression, a

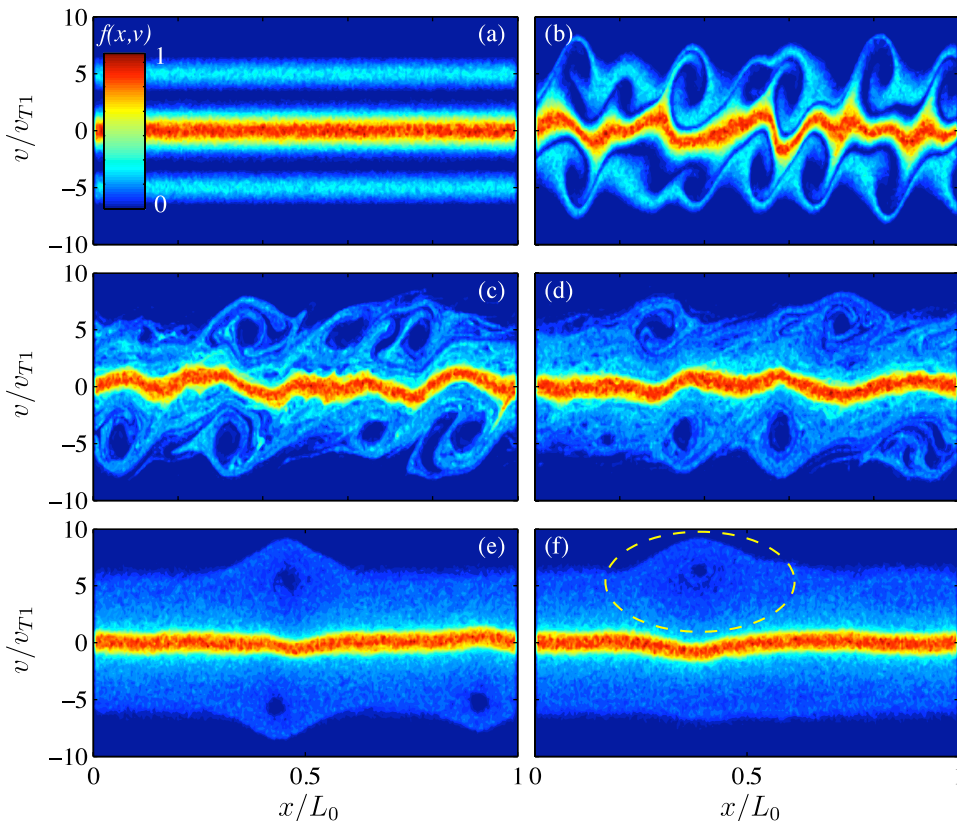


FIG. 2. Snapshots of the electron phase space density  $f(x, v)$  (in arbitrary units) in bounded plasma without compression. These snapshots show the development of the bump-on-tail instability and subsequent evolution of nonlinear BGK-like modes: (a)  $t=0$ , initial bump-on-tail distribution; (b)–(e) formation and merging of electron holes; (f)  $t=280\tau_p$ , final state, corresponding to a solitary electron hole (circled). Time is measured in units  $\tau_p = 2\pi/\omega_p$ . Figure from Ref. 55. Reprinted with permission from P. F. Schmit, I. Y. Dodin, and N. J. Fisch, Phys. Plasmas **18**, 042103 (2011). Copyright 2011 American Institute of Physics.

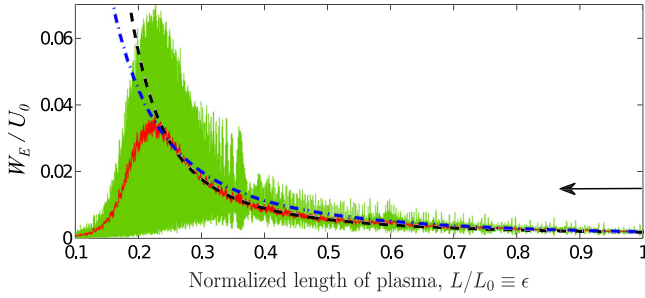


FIG. 3. Evolution of a solitary electron hole during longitudinal compression. Electrostatic energy  $W_E$  normalized to initial plasma total energy  $U_0$ . Pictured are both instantaneous and local time-averaged  $W_E$  (wide and thin line plots, respectively) and also the fitting functions  $W_E/W_{E0} = \epsilon^{-2}$  (dashed-dotted line) and  $W_E/W_{E0} = \exp[2.8(\epsilon^{-1/2} - 1)]$  (dashed line). Note direction of time indicated by arrow. Figure from Ref. 55. Reprinted with permission from P. F. Schmit, I. Y. Dodin, and N. J. Fisch, Phys. Plasmas **18**, 042103 (2011). Copyright 2011 American Institute of Physics.

substantial amount of electron trapping and detrapping is observed, which constitutes a nonadiabatic process and, thus, prevents one from formulating a corresponding ACT for the BGK modes.

The unique behavior of BGK waves in compressing plasma, including their resistance to Landau damping, strong amplification, and ability to persist at high amplitude and relatively slow, thermal phase velocities, suggests that such waves could provide yet another useful tool for targeted phase space engineering in plasma. In addition, there is significant interest in generating and sustaining waves at high  $k\lambda_D$  to be used as an effective grating for the processing of intense laser light in Raman compression studies.<sup>69,70</sup> Compression could provide an additional pathway to access this regime through a part of parameter space that might otherwise be prohibitive.

Further discussion on this topic can be found in Ref. 55.

#### IV. TRANSVERSE NONSTATIONARY PLASMA EFFECTS

The concepts of adiabaticity, action conservation, resonance thresholds, and nonlinearity, in the context of nonstationary plasma evolution, are sufficiently general such that these ideas can be applied across a broad range of wave-plasma systems. Thus, the case of longitudinal 1D compression studied in Sec. III serves primarily as a simple scenario through which each of these fundamental topics could be explored. One might then assume that wave evolution in the presence of perpendicular compression should proceed in a manner very similar to the case of longitudinal compression. This is, to a large extent, a reasonable assumption, but it turns out that perpendicular compression provides access to a regime of nonlinear wave evolution that could not be elicited through longitudinal compression.<sup>71</sup> In the following analysis, note that the exact nature of the compression is inessential, i.e., it can be ballistic or driven by a compressing magnetizing field, for example.

By employing periodic boundary conditions and driving a single electrostatic plasma normal mode with an applied external potential at the linear resonance, one can generate fully phase-mixed nonlinear plasma waves,<sup>72–74</sup> which assume the

identity of an undamped periodic BGK mode when the driver is turned off [Fig. 4(a)]. In the absence of collisions and anisotropy-driven electromagnetic instabilities,<sup>35–38</sup> or on time scales shorter than the characteristic rates for such effects to become significant, perpendicular compression or expansion leads to the scaling,  $\omega_p \propto N^{1/2}$ , much like longitudinal compression, but leaves the parallel thermal velocity  $v_{Te}$  and parallel wave number  $k$  unchanged.<sup>44</sup> Thus, perpendicular compression *increases* the linear plasma wave phase velocity  $u \propto N^{1/2}$ , rather than decreases it (as occurs with longitudinal compression), while leaving the parallel motion of bulk plasma particles unaffected. In this case,  $\kappa \propto N^{-1/2}$ , indicating that collisionless damping is suppressed at all times for compression, making transverse compression qualitatively different from longitudinal compression, where  $\kappa \propto N^{3/2}$ , and induced Landau damping places the dominant limitation on achievable wave amplification (cf. Sec. III).

The increase of  $u$  with perpendicular compression creates a unique set of circumstances from the standpoint of the wave evolution. First, for slow compression, particles that were trapped initially (i.e., when the driver was turned off) are accelerated autoresonantly and remain trapped as the trapped particle phase space island moves to higher velocities [Fig. 4(b)]. Second, because the trapped particle densities are relatively small compared both to the bulk plasma average density and to the bulk plasma fluctuation densities, the wave nonlinearity is initially weak, and the wave approximately conserves the linear action, implying amplification during early stages of compression (cf. Eq. (2)). Since trapped particles conserve their actions, while the total phase space volume of the separatrix increases due to amplification, the trapped particle distribution becomes more deeply trapped with compression [Fig. 4(b)]. It is also worth noting that the expansion of the island separatrix toward lower velocities due to wave amplification is more than offset by

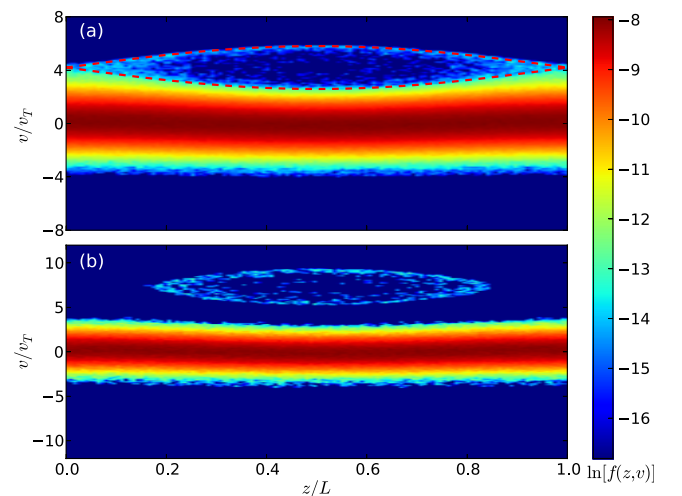


FIG. 4. Snapshots of typical electron distribution,  $f(z, v)$ , associated with nonlinear waves in our PIC simulations. (a) The initial, uncompressed BGK structure after the driver is turned off; dashed red is the separatrix confining trapped electrons. (b) An adiabatically compressed wave; a phase-space island of trapped electrons has been detached from the bulk plasma via autoresonant acceleration. Figure from Ref. 71. Reprinted with permission from P. F. Schmit, I. Y. Dodin, J. Rocks, and N. J. Fisch, Phys. Rev. Lett. **110**, 055001 (2013). Copyright 2013 American Physical Society.

the acceleration of the island average velocity due to the increase in  $u$ . Considering as well that very few particles are found initially at velocities higher than those swept out by the trapped particle island, as can be observed in Fig. 4(a), the wave does not trap additional particles as the plasma is compressed. Hence, the evolution of this nonlinear wave is *truly* adiabatic, since all of the particles in the slowly changing system evolve adiabatically, unlike the BGK modes subjected to longitudinal compression.

This scenario serves as an ideal proving ground to test the recently formulated *nonlinear* action conservation theorem for waves containing trapped particles.<sup>24</sup> Assuming the passing particle response is approximately linear, one can write  $I_{\text{NL}} = I + I_t$ , where  $I$  is just the linear action given in Eq. (1),  $I_t = \int (2\mathcal{W}_t/\omega) d\mathcal{V}$ ,  $\mathcal{W}_t = n_t m u^2/2$  is the energy density of the trapped particle average motion, and  $n_t$  is the trapped particle density averaged over one wave period. Note two remarkable features of this result. First, with the exception of a very minor nonlinear frequency shift,<sup>45,75</sup> the nonlinear action  $I_{\text{NL}}$  is insensitive to the precise shape of the distribution, depending instead only on its average quantities. In addition, part of the wave action,  $I_t$ , is independent of the wave amplitude, which signifies a drastic departure from the conventional picture of nonlinear waves presented in literature.<sup>76</sup>

The amplitude-independent term in  $I_{\text{NL}}$  produces categorical consequences in the nonstationary evolution of waves containing trapped particles. That even small trapped particle populations could become energetically significant makes sense, as their approximate energy density,  $\mathcal{W}_t \propto N^2$ , grows with densification faster than the linear wave energy density,  $\mathcal{W} \propto N^{3/2}$  [cf. Eq. (2)]. By inserting the appropriate parameter scalings into the nonlinear ACT and solving for the amplification gain  $G = \mathcal{W}_E/\mathcal{W}_{E0}$ , one can derive the approximate scaling

$$G \approx N^{3/2} [1 - 2\eta_0(N^{1/2} - 1)], \quad (6)$$

where  $\eta_0 \equiv \mathcal{W}_{t0}/\mathcal{W}_0$  is, remarkably, *the only* parameter that determines the amplification gain for a given compression

ratio  $N$ , up to small nonlinear and thermal corrections. Equation (6) bears a striking resemblance to Eq. (2) for linear waves, but the amplification is attenuated and eventually halted by the second factor, due to the presence of the trapped particle population.

The analytic results demonstrate excellent agreement with PIC simulations, as depicted in Fig. 5(a). One may conclude that significant amplification of nonlinear waves by transverse compression is possible but is limited fundamentally by the initial trapped particle content of the wave. For adiabatic wave evolution, the upper limit for the amplification gain is set by the linear ACT, as observed in the data. Interestingly, once the trapped particle energy content becomes comparable to the rest of the wave energy content, some amount of adiabatic *damping* occurs, at which point deeply trapped particles move closer and closer to the separatrix, until they eventually become detrapped, and the wave evolution can no longer be considered adiabatic [Fig. 5(b)]. A wide variety of nonadiabatic behavior proceeds subsequently, for which the interested reader can find a full discussion in Ref. 71, as well as the recently submitted Ref. 77.

This is the first study of BGK-like wave dynamics in plasma undergoing compression perpendicularly to the wave vector. This paradigmatic problem yields a host of interesting results. First, such compression is found to amplify a wave manyfold, due in large part to the suppression of Landau damping with transverse compression, unlike the case of longitudinal compression in Sec. III. Second, the nonstationary wave evolution conserves nonlinear action, for which our study is the first *ab initio* confirmation. Third, the amplification has an upper limit determined by the total initial energy of the trapped particle average motion but otherwise is insensitive to the particle distribution, and such a limit is always present in theory whenever  $n_t$  is finite. A variety of novel nonadiabatic behavior is also observed. Apart from the academic interest in these new phenomena and the numerical demonstration of the nonlinear ACT, these results suggest yet more ways in which waves can provide new means to manipulate particle phase space and couple energy into plasma.

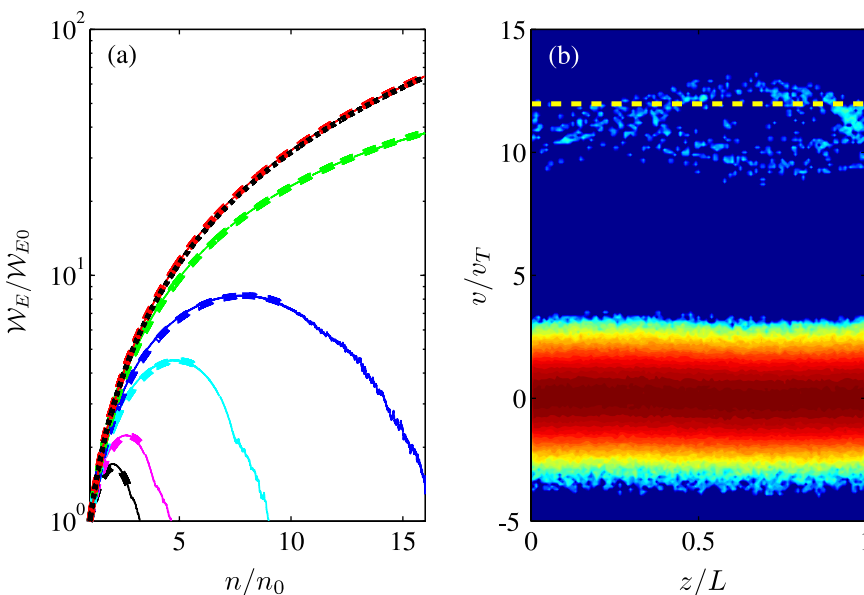


FIG. 5. (a) Amplification gain vs. compression ratio for different  $M_0 \equiv u_0/v_T$ :  $M_0 = 3.8$  (black), 4.0 (magenta), 4.2 (cyan), 4.4 (blue), 4.8 (green), and 6.0 (red). Generally,  $M_0$  and  $\eta_0$  are inversely correlated. Solid are results from PIC simulations, smoothed on the timescales  $\omega_p^{-1}$ . Dashed are Eq. (6) with  $\eta_0$  adjusted to provide the best fit. Dotted, nearly matching the red curve, is the scaling predicted by linear action conservation,  $G \approx N^{3/2}$ . (b) Deteriorating trapped particle island in phase space during wave decay. The dashed line marks the linear phase velocity of the resonant mode,  $\omega_p \Omega/k$ . Since  $u$  exceeds the island average velocity, the wave nonlinear frequency shift is negative, as expected.<sup>45,75</sup> Figure from Ref. 71. Reprinted with permission from P. F. Schmit, I. Y. Dodin, J. Rocks, and N. J. Fisch, Phys. Rev. Lett. **110**, 055001 (2013). Copyright 2013 American Physical Society.

## V. APPLICATIONS

While the ultimate goal of this work is to draw useful connections to modern ICF research, two applications immediately lend themselves to the present study of Langmuir waves in nonstationary plasma. These applications include wave-induced current drive in nonstationary plasma as well as a new plasma-based particle acceleration scheme employing plasma compression as a means to exert control over the accelerating wave dynamics.

### A. Current drive in nonstationary plasma

One application that immediately lends itself to the results obtained in this work is wave-induced current drive. The problem of driving electrical currents in plasma using waves is well studied in the context of stationary, magnetically-confined plasma.<sup>5</sup> Since the goal of wave-driven current drive is to create conditions that favor steady-state reactor operation, most current drive calculations are similarly steady-state in nature. The problem of driving current in nonstationary plasma is inherently non-steady-state and warrants a careful treatment, leading to unique effects not present in stationary plasma. Two separate studies have examined current drive in two different nonstationary scenarios: plasma undergoing charge recombination<sup>78</sup> and plasma undergoing perpendicular expansion and compression.<sup>79</sup>

Driving electrical current in plasma using waves requires the injection of waves that interact preferentially with a single plasma species to generate a velocity space anisotropy through wave-particle resonance.<sup>5</sup> This anisotropy can result in a net electrical current, which must compete with the effects of collisional isotropization in order to persist, requiring continuous injection of wave energy to operate in the steady-state. Often, the wave-particle interactions selected for current drive target suprathermal electrons due to their reduced collisionality. Thus, collisions play an important role in the calculation of the overall efficiency of a current drive scenario, and in nonstationary plasma, the relative strength of collisional effects can vary significantly.

The case of plasma undergoing charge recombination provides a useful paradigmatic nonstationary system in which to study the collisional relaxation of particle velocity space anisotropies in the context of current drive.<sup>78</sup> Remarkably, the Langevin equations, taken in the strict high-velocity limit to describe the relaxation of suprathermal electrons,<sup>5,80,81</sup> admit an exact analytical solution for plasma exhibiting time-varying charged particle number densities due to charge recombination. One can derive the current density produced by arbitrary particle fluxes, from which the current drive efficiency can be calculated and optimized both for discrete and continuous pulses of wave energy. One interesting and ubiquitous feature in recombining plasma is the existence of a non-zero *residual* current density that persists time-asymptotically under certain conditions, a feature not present in stationary plasma. Though the model neglects other dissipative forces that would eventually quench a current, such as collisions with neutrals or recombination of the suprathermal current carriers, the results suggest that current could be prolonged substantially in plasma with time-varying bulk properties.

Further discussion on this topic can be found in Ref. 78.

Explicit PIC simulations of current drive in nonstationary plasma were carried out in the case of perpendicularly expanding and compressing plasma. In this case, a magnetized plasma preseeded with an initially undamped Langmuir wave transitions to a collisionless damping regime in a switchlike manner upon expansion of the plasma perpendicular to the background magnetic field. Recall from Sec. IV that transverse compression and expansion gives  $\kappa \propto N^{-1/2}$ , from which it is clear that expansion is required to induce Landau damping. Because the linear Langmuir wave carries no momentum initially, and Landau damping conserves total momentum, velocity-dependent collisions between electrons and ions are required in order for an electric current to arise.<sup>4</sup> Since particle collision rates  $\nu_c \propto 1/v^3$ , the enhanced anisotropic high energy electron tail resulting from induced Landau damping leads to a net electrical current. The sudden rise in electrical current also induces a voltage within the plasma due to  $L/R$  effects associated with the specific plasma geometry.

The current drive efficiency of this effect in nonstationary plasma is shown to depend on the rate of plasma expansion, which determines both the onset and extent of the collisionless damping as well as the time-varying strength of particle collisions, and the plasma  $L/R$  time. Figure 6 shows the electron parallel velocity distributions vs. time for two different rates of expansion. At the faster expansion rate [Fig. 6(a)], enhanced particle trapping by the wave modifies significantly the suprathermal electron distribution in the vicinity of the resonance,<sup>47,82</sup> accelerating electrons to

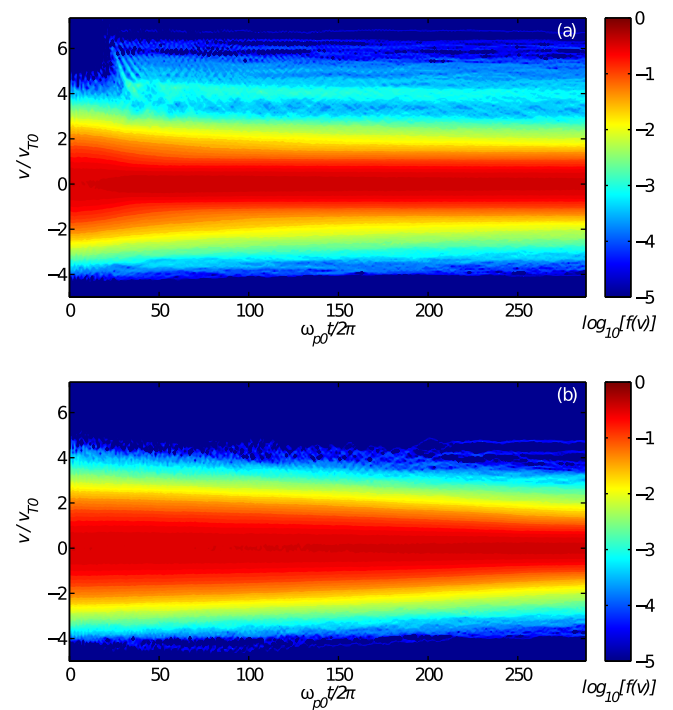


FIG. 6. Plot of  $\log_{10}[f(v,t)]$ , with  $f(v,t)$  the electron parallel velocity distribution function, for (a)  $T = 30\tau_{p0}$  and (b)  $T = 250\tau_{p0}$ , with  $T$  is the total magnetic expansion time and  $\tau_{p0} = 2\pi/\omega_{p0}$ . Cooling of bulk parallel velocities is due to collisional coupling with perpendicular velocities. Figure from Ref. 79. Reprinted with permission from P. F. Schmit and N. J. Fisch, Phys. Rev. Lett. **108**, 215003 (2012). Copyright 2012 American Physical Society.

higher parallel velocities by amounts comparable to the Langmuir wave trapping width,  $v_{tr} \equiv 2\omega_b/k$ . On the other hand, Fig. 6(b) indicates that slower expansion leads to less particle trapping, thus limiting the production of high-energy electrons. It is found that faster expansion rates generally lead to more prolonged currents, owing to the enhanced flux of current-carrying electrons to higher velocities, and hence, the formation of lower collisionality configurations. It is also found that subsequent recompression of the plasma enhances the current drive effect by increasing particle perpendicular energies, and hence, reducing further the collision rates of the current-carrying electrons.

Further discussion on this topic can be found in Ref. 79.

## B. Plasma-based particle acceleration with magnetic compression

Charged-particle acceleration in plasma typically employs short, intense laser pulses or high energy electron beams to drive high amplitude plasma waves capable of accelerating relativistic particles to high energies over very short distances.<sup>84–88</sup> One effect that significantly limits the attainable gain in plasma-based accelerators is *phase slippage*, in which a particle eventually overtakes the segment of the wave providing a positive accelerating force (see, e.g., Ref. 86). Some methods to improve electron energy gain attempt to keep an accelerating electron in phase with the wave for an extended period of time, achieving this goal, e.g., by means of an applied transverse magnetic field<sup>89,90</sup> or a stationary axial density gradient.<sup>91–95</sup>

In the scheme considered here, the use of a modest [ $\mathcal{O}(10\text{ kG})$ ] axial, time-varying magnetic field in the acceleration channel is proposed as a method to overcome electron dephasing.<sup>83</sup> The evolution of the uniform axial magnetic field leads to plasma densification, enabling direct, time-resolved control of the plasma wave properties, particularly through the dependence of the phase velocity on the plasma density,  $u \propto n^{1/2}$ . This general methodology can be applied to the leading acceleration approaches; however, the compression profile required to maximize energy gain varies significantly between plasma beat-wave (PBWA) techniques and wakefield techniques, including plasma wakefield acceleration (PWFA) and laser wakefield acceleration (LWFA). Static axial magnetic fields have already been shown to provide performance benefits in plasma-based acceleration,<sup>96–99</sup> yet this is the first time a time-varying field is proposed as a precise control mechanism for the plasma wave dynamics.

For PBWA, only a small fractional density increase via compression is needed to increase the electron dephasing characteristic length to arbitrarily long distances, and no cross-beam electron transport is induced, unlike the surfatron.<sup>89</sup> For wakefield acceleration, the density increase required for uniform plasma compression is compared to the axial density gradient technique, and the resulting density profiles demonstrate a much more gradual characteristic rise in the case of uniform compression. Figure 7 displays the optimized 1D density profiles corresponding to each method. The stationary density gradient profile spans many orders of magnitude, becoming singular near the point where the

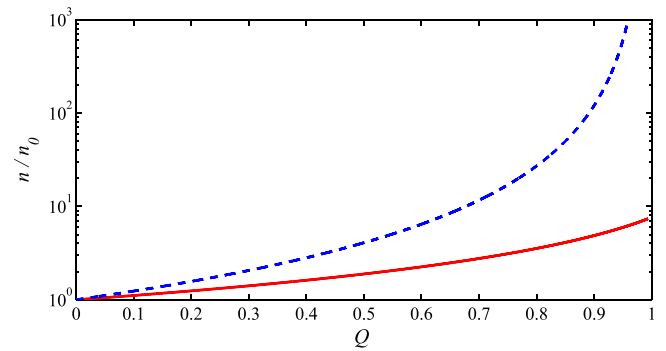


FIG. 7. Optimized density profiles to address wakefield dephasing for (a) the axial density gradient method (dashed line), with  $Q = z/L$  signifying an axially inhomogeneous density profile, and (b) the perpendicular magnetic compression method (solid line), with  $Q = t/T$  signifying a time-varying, but axially uniform, density profile. Note that  $L = cT$ , and accelerating electrons initialized identically in each case will overtake the driver pulse after the same time  $T$  and path length  $L$  in both cases. Figure from Ref. 83. Reprinted with permission from P. F. Schmit and N. J. Fisch, Phys. Rev. Lett. **109**, 255003 (2012). Copyright 2012 American Physical Society.

accelerating electrons overtake the driver (after time  $T$  over length  $L = cT$ ). Uniform compression achieves proper wave-particle phasing over a similar time and distance, but it does so utilizing a much smaller shift in plasma density. For PWFA, uniform compression can also increase the amplitude of the wakefield with distance, unlike the axial density gradient method.

The physical mechanism underlying this result is related to the time-variation of the bulk plasma, which causes the wakefield properties to continue evolving after the driver pulse has passed, but before the accelerating electron bunch catches up. Besides the performance enhancement arising from dephasing, it is also possible that generating a time-varying, uniform density profile with magnetic compression could be technologically easier than generating an enormous stationary plasma density gradient over relatively short [ $\mathcal{O}(\text{cm})$ ] distances.

Further discussion on this topic can be found in Ref. 83.

## VI. CONCLUSIONS

Here, we reviewed recent findings pertaining to the dynamics of waves in nonstationary plasma. In seeking to describe the entire life cycle of a plasma wave embedded in nonstationary, collisional plasma, a number of interesting and novel results were uncovered. In plasma undergoing compression, embedded waves can have very unusual and possibly useful properties. For example, part of the mechanical energy of compressing plasma can be transferred controllably to hot electrons by seeding the plasma with plasma waves. Under compression, wherein wave action is conserved initially, both linearly and nonlinearly, the wave energy grows as its frequency and wavenumber change adiabatically, until suddenly, the wave damps, resulting in switchlike production not only of heat but also voltage and current. These bursts can be controlled precisely in time by prescribing the compression script. Several classic problems in wave physics, including the bump-on-tail instability and nonlinear BGK waves, exhibit new effects under compression. In addition, the wavelike

perturbations undergoing compression or expansion affect fundamental bulk properties of the plasma, such as the plasma compressibility; moreover, and rather remarkably, nonlinear waves, such as BGK modes, affect the plasma compressibility differently. The dynamics of such nonlinear modes are influenced significantly by the presence of trapped particles. Wave-particle interactions mediated by plasma compression also can enhance the performance of plasma-based particle accelerators. To describe numerically all these effects, novel particle-in-cell (PIC) simulations were developed. These findings point towards potentially beneficial applications, including in ICF and HED physics, where extreme compression is exercised on dense plasma, which could be seeded with waves.

## ACKNOWLEDGMENTS

This work was supported by the U.S. Defense Threat Reduction Agency, the DOE under Contract No. DE-AC02-09CH11466, and by the NNSA SSAA Program through DOE Research Grant No. DE-FG52-08NA28553. One of us (P.F.S.) was also supported by the National Defense Science and Engineering Graduate (NDSEG) Fellowship during a portion of the period in which the research was conducted.

- <sup>1</sup>K. Appert, T. Hellsten, O. Sauter, S. Succi, J. Vaclavik, and L. Villard, *Comput. Phys. Commun.* **43**, 125 (1986).
- <sup>2</sup>V. E. Golant and V. I. Fedorov, *RF Plasma Heating in Toroidal Fusion Devices* (Plenum, 1989).
- <sup>3</sup>A. G. Litvak, G. V. Permitin, E. V. Suvorov, and A. A. Frajman, *Nucl. Fusion* **17**, 659 (1977).
- <sup>4</sup>N. J. Fisch and A. H. Boozer, *Phys. Rev. Lett.* **45**, 720 (1980).
- <sup>5</sup>N. J. Fisch, *Rev. Mod. Phys.* **59**, 175–234 (1987).
- <sup>6</sup>N. J. Fisch and J. M. Rax, *Phys. Rev. Lett.* **69**, 612 (1992).
- <sup>7</sup>N. J. Fisch and J. M. Rax, *Phys. Fluids B* **5**, 1754 (1993).
- <sup>8</sup>N. J. Fisch, *Phys. Rev. Lett.* **97**, 225001 (2006).
- <sup>9</sup>A. J. Fetterman and N. J. Fisch, *Phys. Rev. Lett.* **101**, 205003 (2008).
- <sup>10</sup>A. I. Zhmoginov and N. J. Fisch, *Phys. Plasmas* **16**, 112511 (2009).
- <sup>11</sup>T. C. Sangster, R. L. McCrory, V. N. Goncharov, D. R. Harding, S. J. Loucks, P. W. McKenty, D. D. Meyerhofer, S. Skupsky, B. Yaakobi, B. J. MacGowan *et al.*, *Nucl. Fusion* **47**, S686 (2007).
- <sup>12</sup>E. I. Moses, *Nucl. Fusion* **49**, 104022 (2009).
- <sup>13</sup>D. D. Ryutov, M. S. Derzon, and M. K. Matzen, *Rev. Mod. Phys.* **72**, 167 (2000).
- <sup>14</sup>M. K. Matzen, M. A. Sweeney, R. G. Adams, J. R. Asay, J. E. Bailey, G. R. Bennett, D. E. Bliss, D. D. Bloomquist, T. A. Brunner, R. B. Campbell *et al.*, *Phys. Plasmas* **12**, 055503 (2005).
- <sup>15</sup>S. A. Slutz, M. C. Herrmann, R. A. Vesey, A. B. Sefkow, D. B. Sinars, D. C. Rovang, K. J. Peterson, and M. E. Cuneo, *Phys. Plasmas* **17**, 056303 (2010).
- <sup>16</sup>H. S. Hudson, *Solar Phys.* **133**, 357 (1991).
- <sup>17</sup>R. P. Lin and H. S. Hudson, *Solar Phys.* **50**, 153 (1976).
- <sup>18</sup>J. A. Miller, P. J. Cargill, A. G. Emslie, G. D. Holman, B. R. Dennis, T. N. LaRosa, R. M. Winglee, S. G. Benka, and S. Tsuneta, *J. Geophys. Res.* **102**, 14631, doi:10.1029/97JA00976 (1997).
- <sup>19</sup>B. Roberts, *Solar Phys.* **193**, 139 (2000).
- <sup>20</sup>E. Liang, K. Nishimura, H. Li, and S. P. Gary, *Phys. Rev. Lett.* **90**, 085001 (2003).
- <sup>21</sup>A. G. Sgro, S. P. Gary, and D. S. Lemons, *Phys. Fluids B* **1**, 1890 (1989).
- <sup>22</sup>S. H. Brecht, D. W. Hewett, and D. J. Larson, *Geophys. Res. Lett.* **36**, L15105, doi:10.1029/2009GL038393 (2009).
- <sup>23</sup>D. W. Hewett, S. H. Brecht, and D. J. Larson, *J. Geophys. Res.* **116**, A11310, doi:10.1029/2011JA016904 (2011).
- <sup>24</sup>I. Y. Dodin and N. J. Fisch, *Phys. Plasmas* **19**, 012102 (2012).
- <sup>25</sup>A. V. Bobylev and K. Nanbu, *Phys. Rev. E* **61**, 4576 (2000).
- <sup>26</sup>M. E. Jones, D. S. Lemons, R. J. Mason, V. A. Thomas, and D. Winske, *J. Comp. Phys.* **123**, 169 (1996).
- <sup>27</sup>W. M. Manheimer, M. Lampe, and G. Joyce, *J. Comp. Phys.* **138**, 563 (1997).
- <sup>28</sup>D. J. Larson, *J. Comp. Phys.* **188**, 123 (2003).
- <sup>29</sup>D. S. Lemons, D. Winske, W. Daughton, and B. Albright, *J. Comp. Phys.* **228**, 1391 (2009).
- <sup>30</sup>B. I. Cohen, A. M. Dimits, and D. J. Strozzi, *J. Comp. Phys.* **234**, 33 (2013).
- <sup>31</sup>K. Nanbu, *Phys. Rev. E* **55**, 4642 (1997).
- <sup>32</sup>C. Wang, T. Lin, R. Caffisch, B. I. Cohen, and A. M. Dimits, *J. Comp. Phys.* **227**, 4308 (2008).
- <sup>33</sup>A. M. Dimits, C. Wang, R. Caffisch, B. I. Cohen, and Y. Huang, *J. Comp. Phys.* **228**, 4881 (2009).
- <sup>34</sup>C. K. Birdsall and A. B. Langdon, *Plasma Physics via Computer Simulation* (Taylor & Francis, 2005), paperback ed.
- <sup>35</sup>S. P. Gary, M. D. Montgomery, W. C. Feldman, and D. W. Forslund, *J. Geophys. Res.* **81**, 1241, doi:10.1029/JA081i007p01241 (1976).
- <sup>36</sup>S. P. Gary and C. D. Madland, *J. Geophys. Res.* **90**, 7607, doi:10.1029/JA090iA08p07607 (1985).
- <sup>37</sup>S. P. Gary and J. Wang, *J. Geophys. Res.* **101**, 10749, doi:10.1029/96JA00323 (1996).
- <sup>38</sup>S. P. Gary, K. Liu, and D. Winske, *Phys. Plasmas* **18**, 082902 (2011).
- <sup>39</sup>P. F. Schmit, I. Y. Dodin, and N. J. Fisch, *Phys. Rev. Lett.* **105**, 175003 (2010).
- <sup>40</sup>G. B. Whitham, *J. Fluid Mech.* **22**, 273 (1965).
- <sup>41</sup>R. L. Dewar, *J. Plasma Phys.* **7**, 267 (1972).
- <sup>42</sup>Y. A. Kravtsov, L. A. Ostrovsky, and N. S. Stepanov, *Proc. IEEE* **62**, 1492 (1974).
- <sup>43</sup>I. B. Bernstein, *Phys. Fluids* **18**, 320 (1975).
- <sup>44</sup>I. Y. Dodin, V. I. Geyko, and N. J. Fisch, *Phys. Plasmas* **16**, 112101 (2009).
- <sup>45</sup>I. Y. Dodin and N. J. Fisch, *Phys. Rev. Lett.* **107**, 035005 (2011).
- <sup>46</sup>T. H. Stix, *Waves in Plasmas* (American Institute of Physics, 1992), Chap. VIII.
- <sup>47</sup>T. O'Neil, *Phys. Fluids* **8**, 2255 (1965).
- <sup>48</sup>P. F. Schmit, C. R. Mooney, I. Y. Dodin, and N. J. Fisch, *J. Plasma Phys.* **77**, 629 (2011).
- <sup>49</sup>I. Y. Dodin and N. J. Fisch, *Phys. Lett. A* **374**, 3472 (2010).
- <sup>50</sup>G. W. Kentwell and D. A. Jones, *Phys. Rep.* **145**, 319 (1987).
- <sup>51</sup>N. A. Krall and A. W. Trivelpiece, *Principles of Plasma Physics*, 1st ed. (McGraw-Hill, 1973), Chap. 10.
- <sup>52</sup>F. Reif, *Fundamentals of Statistical and Thermal Physics* (McGraw-Hill, Inc., 1965), Sec. 5.7.
- <sup>53</sup>C. S. Gardner, *Phys. Fluids* **6**, 839 (1963).
- <sup>54</sup>I. Y. Dodin and N. J. Fisch, *Phys. Lett. A* **341**, 187 (2005).
- <sup>55</sup>P. F. Schmit, I. Y. Dodin, and N. J. Fisch, *Phys. Plasmas* **18**, 042103 (2011).
- <sup>56</sup>I. Bernstein, J. M. Greene, and M. D. Kruskal, *Phys. Rev.* **108**, 546 (1957).
- <sup>57</sup>W. Bertsche, J. Fajans, and L. Friedland, *Phys. Rev. Lett.* **91**, 265003 (2003).
- <sup>58</sup>H. Schamel, *Phys. Plasmas* **7**, 4831 (2000) and references therein.
- <sup>59</sup>H. Schamel, *Phys. Plasmas* **19**, 020501 (2012).
- <sup>60</sup>H. L. Berk, C. E. Nielsen, and K. V. Roberts, *Phys. Fluids* **13**, 980 (1970).
- <sup>61</sup>K. Saeki, P. Michelsen, H. L. Pécseli, and J. J. Rasmussen, *Phys. Rev. Lett.* **42**, 501 (1979).
- <sup>62</sup>M. M. Shoucri, *Phys. Fluids* **22**, 2038 (1979).
- <sup>63</sup>T. H. Dupree, *Phys. Fluids* **25**, 277 (1982).
- <sup>64</sup>L. Demeio and P. F. Zweifel, *Phys. Fluids B* **2**, 1252 (1990).
- <sup>65</sup>H. L. Berk, B. N. Breizman, and N. V. Petviashvili, *Phys. Lett. A* **234**, 213 (1997); **238**, 408 (1998).
- <sup>66</sup>K. V. Roberts and H. L. Berk, *Phys. Rev. Lett.* **19**, 297 (1967).
- <sup>67</sup>M. V. Goldman, *Phys. Fluids* **13**, 1281 (1970).
- <sup>68</sup>V. B. Krapchev and A. K. Ram, *Phys. Rev. A* **22**, 1229 (1980).
- <sup>69</sup>V. M. Malkin, G. Shvets, and N. J. Fisch, *Phys. Rev. Lett.* **82**, 4448 (1999).
- <sup>70</sup>V. M. Malkin, N. J. Fisch, and J. S. Wurtele, *Phys. Rev. E* **75**, 026404 (2007).
- <sup>71</sup>P. F. Schmit, I. Y. Dodin, J. Rocks, and N. J. Fisch, *Phys. Rev. Lett.* **110**, 055001 (2013).
- <sup>72</sup>L. Friedland, P. Khain, and A. G. Shagalov, *Phys. Rev. Lett.* **96**, 225001 (2006).
- <sup>73</sup>F. Valentini, T. M. O'Neil, and D. H. E. Dubin, *Phys. Plasmas* **13**, 052303 (2006).
- <sup>74</sup>J. W. Banks, R. L. Berger, S. Brunner, B. I. Cohen, and J. A. F. Hittinger, *Phys. Plasmas* **18**, 052102 (2011).
- <sup>75</sup>I. Y. Dodin and N. J. Fisch, *Phys. Plasmas* **19**, 012103 (2012).

- <sup>76</sup>G. B. Whitham, *Linear and Nonlinear Waves* (Wiley, New York, 1974), Chaps. 14 and 15.
- <sup>77</sup>I. Y. Dodin, P. F. Schmit, J. Rocks, and N. J. Fisch, "Negative-mass instability in nonlinear plasma waves," Phys. Rev. Lett. (unpublished).
- <sup>78</sup>P. F. Schmit and N. J. Fisch, *Phys. Plasmas* **18**, 102102 (2011).
- <sup>79</sup>P. F. Schmit and N. J. Fisch, *Phys. Rev. Lett.* **108**, 215003 (2012).
- <sup>80</sup>S. Chandrasekhar, *Rev. Mod. Phys.* **15**, 1 (1943).
- <sup>81</sup>M. C. Wang and G. E. Uhlenbeck, *Rev. Mod. Phys.* **17**, 323 (1945).
- <sup>82</sup>G. Manfredi, *Phys. Rev. Lett.* **79**, 2815 (1997).
- <sup>83</sup>P. F. Schmit and N. J. Fisch, *Phys. Rev. Lett.* **109**, 255003 (2012).
- <sup>84</sup>T. Tajima and J. M. Dawson, *Phys. Rev. Lett.* **43**, 267 (1979).
- <sup>85</sup>M. Everett, A. Lal, D. Gordon, C. E. Clayton, K. A. Marsh, and C. Joshi, *Nature* **368**, 527 (1994).
- <sup>86</sup>E. Esarey, P. Sprangle, J. Krall, and A. Ting, *IEEE Trans. Plasma Sci.* **24**, 252 (1996).
- <sup>87</sup>E. Esarey, C. B. Schroeder, and W. P. Leemans, *Rev. Mod. Phys.* **81**, 1229 (2009).
- <sup>88</sup>R. Bingham, J. T. Mendonça, and P. K. Shukla, *Plasma Phys. Controlled Fusion* **46**, R1 (2004).
- <sup>89</sup>T. Katsouleas and J. M. Dawson, *Phys. Rev. Lett.* **51**, 392 (1983).
- <sup>90</sup>J. Vieira, S. F. Martins, V. B. Pathak, R. A. Fonseca, W. B. Mori, and L. O. Silva, *Phys. Rev. Lett.* **106**, 225001 (2011).
- <sup>91</sup>T. Katsouleas, *Phys. Rev. A* **33**, 2056 (1986).
- <sup>92</sup>P. Sprangle, B. Hafizi, J. R. Peñano, R. F. Hubbard, A. Ting, A. Zigler, and J. T. M. Antonsen, *Phys. Rev. Lett.* **85**, 5110 (2000).
- <sup>93</sup>A. Pukhov and I. Kostyukov, *Phys. Rev. E* **77**, 025401 (2008).
- <sup>94</sup>C. G. R. Geddes, K. Nakamura, G. R. Plateau, C. Toth, E. Cormier-Michel, E. Esarey, C. B. Schroeder, J. R. Cary, and W. P. Leemans, *Phys. Rev. Lett.* **100**, 215004 (2008).
- <sup>95</sup>W. Rittershofer, C. B. Schroeder, E. Esarey, F. J. Grüner, and W. P. Leemans, *Phys. Plasmas* **17**, 063104 (2010).
- <sup>96</sup>T. Hosokai, K. Kinoshita, A. Zhidkov, A. Maekawa, A. Yamazaki, and M. Uesaka, *Phys. Rev. Lett.* **97**, 075004 (2006).
- <sup>97</sup>M. S. Hur, D. N. Gupta, and H. Suk, *Phys. Lett. A* **372**, 2684 (2008).
- <sup>98</sup>D. H. Froula, L. Divol, P. Davis, J. P. Polastro, P. Michel, V. Leurent, S. H. Glenzer, B. B. Pollock, and G. Tynan, *Plasma Phys. Controlled Fusion* **51**, 024009 (2009).
- <sup>99</sup>R. Prasad, R. Singh, and V. K. Tripathi, *Laser Part. Beams* **27**, 459 (2009).